

OPEN

# A simulation-based comparative study of glaucoma filtration surgeries using computational fluid dynamics

Nicol Basson, PhDa,b,\*D, Patrick Geoghegan, PhDc,d, Susan Williams, MD, PhDe, Weihua Ho, PhDb,f,g

## **Abstract**

Computational fluid dynamics (CFD) offers a virtual platform to assess glaucoma surgeries, predicting intraocular pressure (IOP) outcomes. CFD shows that modified nonpenetrating deep sclerectomy (mNPDS) achieves IOP reduction comparable to trabeculectomy, guiding surgical decisions and innovations. Effective solutions for glaucoma surgical treatment represent a significant challenge in ophthalmology. The advent of numerous techniques in the last decade has complicated the evaluation of competing methodologies, typically addressed through costly and time-consuming randomized controlled clinical trials. This study explores an alternative approach using CFD to virtually assess the flow and IOP effects of glaucoma surgical procedures. A 3D model of an idealized anterior eye segment was created as a means to directly compare various glaucoma filtration surgical procedures. The CFD model was specifically utilized to compare trabeculectomy, nonpenetrating deep sclerectomy (NPDS) without the removal of the juxtacanalicular trabecular meshwork (JCT), and mNPDS including the JCT peel. The CFD results reveal that NPDS alone is less effective than trabeculectomy in lowering IOP at the time of surgery. The postoperative IOP was 7 mm Hg for trabeculectomy and 23.4 mm Hg for NPDS. However, the mNPDS procedure produced IOP results comparable to that of trabeculectomy, with a postoperative IOP of 6.98 mm Hg. An interesting additional finding in trabeculectomy is the low flows at the corneal wall. This flow pattern is not seen with NPDS and may partially explain the better safety profile of NPDS compared with trabeculectomy. While CFD does not replace clinical trials, this study underscores its potential in virtually evaluating glaucoma surgical procedures.

**Abbreviations:** CFD = computational fluid dynamics, IOP = intraocular pressure, JCT = juxtacanalicular tissue, mNPDS = modified nonpenetrating deep sclerectomy, NPDS = nonpenetrating deep sclerectomy, TM = trabecular meshwork, SC = Schlemm canal.

Keywords: computational fluid dynamics, glaucoma, intraocular pressure, nonpenetrating deep sclerectomy, trabeculectomy

## 1. Introduction

Advancements in glaucoma treatments constantly introduce new surgical techniques, but direct comparisons remain challenging, often requiring costly and time-intensive randomized controlled trials. These delays hinder timely evaluations of new procedures. The cost and time associated with such trials delay result evaluation until several years after the introduction of new procedures.

Intraocular pressure (IOP) is intricately linked to aqueous humor flow in the eye and poses a critical aspect of glaucoma treatment. Currently, aqueous humor flow is not fully understood, and an improved comprehension of the subject could help to improve glaucoma treatment options.<sup>[1]</sup> Computational fluid dynamics (CFD) is a software tool that uses mathematical modeling to simulate fluid flow phenomena. The models used in CFD studies are governed by fluid property relations and boundary conditions. The solution for the CFD model itself is solved by means of the Navier–Stokes equations, which evaluate the mass, energy, and momentum conservations of a thermofluid system. While CFD has been

This research was partially funded by the National Research Foundation (Thuthuka grant). The funder had no role in study design, data collection, analysis, or manuscript preparation.

The authors have no conflicts of interest to disclose.

The datasets generated during and/or analyzed during the current study are not publicly available, but are available from the corresponding author on reasonable request.

<sup>a</sup> Department of Thermal and Fluid Engineering, Faculty Engineering Technology, University of Twente, Enschede, The Netherlands, <sup>b</sup> School of Mechanical, Industrial & Aeronautical Engineering, Faculty of Engineering & the Built Environment, University of Witwatersrand, Johannesburg, South Africa, <sup>c</sup> Department of Mechatronics & Biomedical Engineering, School of Engineering & Innovation, College of Engineering & Physical Sciences, Aston University, Birmingham, United Kingdom, <sup>a</sup> Aston Fluids Group, Aston University, Birmingham, United Kingdom, <sup>a</sup> School of Clinical Medicine, Faculty of Health Sciences, University of the Witwatersrand, Johannesburg, South Africa, <sup>1</sup> The Centre for Research in Computational and Applied Mechanics, University of

Cape Town, Cape Town, South Africa, <sup>9</sup> Department of Mechanical Engineering, University of Cape Town, Cape Town, South Africa.

\* Correspondence: Nicol Basson, Department of Thermal and Fluid Engineering, Faculty Engineering Technology, University of Twente, Drienerlolaan 5, 7522 NB Enschede, The Netherlands (e-mail: n.basson@utwente.nl).

Copyright © 2025 the Author(s). Published by Wolters Kluwer Health, Inc. This is an open-access article distributed under the terms of the Creative Commons Attribution-Non Commercial License 4.0 (CCBY-NC), where it is permissible to download, share, remix, transform, and buildup the work provided it is properly cited. The work cannot be used commercially without permission from the journal.

How to cite this article: Basson N, Geoghegan P, Williams S, Ho W. A simulation-based comparative study of glaucoma filtration surgeries using computational fluid dynamics. Medicine 2025;XX:XX(e45678).

Received: 10 July 2025 / Received in final form: 29 September 2025 / Accepted: 3 October 2025

http://dx.doi.org/10.1097/MD.000000000045678

employed in studies on glaucomatous aqueous humor flow and retinal diseases,<sup>[2-5]</sup> its application to the in-depth study of glaucoma drainage surgeries has been limited. Compared to alternative studies like *ex vivo* eye models, CFD also offers control over boundary conditions, standardization of anatomical geometries, and the elimination of biological variability. These features make CFD particularly well-suited for isolating and comparing the fluid dynamic effects of different surgical modifications.

We hypothesized that CFD could be used as an *in silico* solution for studying and evaluating these procedures. The procedures we elected to compare are trabeculectomy and non-penetrating deep sclerectomy NPDS.

Trabeculectomy is considered the "gold standard" for successfully reducing IOP in patients with open-angle glaucoma (OAG). [6,7] Despite its success, trabeculectomy is associated with complications such as wound leaks, hypotony, and cataract development.[8-12] In recent years, safer alternatives to trabeculectomy have been suggested. Nonpenetrating deep sclerectomy (NPDS) is a less invasive version of trabeculectomy that has been suggested to be just as effective for treating OAG.[9,13,14] However, the effectiveness of NPDS is still being debated, as some studies suggest that it has a lower efficacy profile than that of trabeculectomy. [10,15] To overcome this, modified NPDS (mNPDS) procedures have become more widely used, which includes removing the juxtacanalicular trabecular meshwork (JCT).[16] This mNPDS procedure occurs after deroofing the canal of Schlemm and is also known as the removal of the inner wall of Schlemm canal (SC) or simply as a "membrane peel." The JCT part of the trabecular meshwork (TM) causes the highest resistance to aqueous humor outflow due to its low porosity. Both clinical and mathematical studies have suggested that the membrane peel is key to the success of the NPDS procedure. [17-19] Several studies suggest that mNPDS can reduce IOP to a standard that is comparable with trabeculectomy,[11,20,21] but others still claim that this is not the case. [8,22,23] In general, the discussion around the pressurereducing effects of NPDS compared to trabeculectomy is still controversial, causing hesitation in adopting NPDS as a safe alternative to trabeculectomy.[18,19]

The objective of this study was to compare the impact of trabeculectomy, NPDS, and mNPDS on identical idealized eye geometries using CFD. The primary parameters for evaluation include IOP and its immediate postoperative reduction rate. While CFD has been used in ophthalmology to model various aspects of aqueous humor dynamics, [5,24] no previous studies have directly compared the fluidic outcomes of trabeculectomy, NPDS, and mNPDS in a standardized computational framework. This study addresses that gap by simulating and comparing their immediate postoperative effects on IOP. This exploration seeks to provide insights into the efficacy of these glaucoma surgeries in terms of IOP reduction, setting the stage for potential future investigations with a focus on computational modeling for surgical procedure studies.

# 2. Methods

This study is a comparative *in silico* simulation analysis using CFD to model and evaluate immediate postoperative IOP following 3 types of glaucoma filtration surgeries. Ethical review and informed consent were not required since all data used in the computational modeling were derived from open-access sources. The competing filtration surgeries were simulated using an idealized 3D model of the human eye. The benefit of this approach is that the eye geometry is identical for both simulations and there are no interfering parameters (e.g., previous eye conditions or surgeries) that may affect the results. Three cases are presented: trabeculectomy, NPDS and mNPDS. In the case of

the mNPDS procedure, the JCT layer is removed in addition to deroofing the canal of Schlemm. For each simulated surgical scenario, IOP was the primary outcome variable. The surgical modification (e.g., trabeculectomy, NPDS, mNPDS) functioned as the exposure condition. To minimize bias across surgical scenarios, all simulations were conducted using identical eye geometry, boundary conditions, and fluid properties. Potential sources of bias, including the exclusion of patient-specific anatomical variations and biological healing responses, are addressed in Section 4.

### 2.1. Study design and governing equations

For the computational model, the flow domain geometry of the anterior eye segment was created in Autodesk Inventor® 2021 (Autodesk Inc., San Francisco). The flow domain represents the space where the fluid flow takes place. Thus, no physical walls are modeled. The anterior segment flow domain consists of the pupil, the anterior chamber, the TM, the SC, and the collector channels. Following this, the aqueous humor dynamics within the eye were simulated using Ansys Fluent 2021 R2. Figure 1 depicts the flow domain (gray) as it is extracted from the ideal eye geometry, together with its aqueous fluid inlet (blue) and outlets (red). The resistance of the TM (green) is simulated using Darcy Law. For an open-angle glaucomatous setup, the permeability was calculated to be 4.34E-16 m<sup>2</sup> to achieve an IOP of 27 mm Hg. For typical aqueous humor production in the ciliary body, the inlet boundary condition at the pupil is a mass flow rate of 5E-08 kg/s (3 μL/min). The outlet channels have a pressure boundary of 7 mm Hg.[3]

The aqueous humor fluid properties have a density of  $1000\,\text{kg/m}^3$  and dynamic viscosity ( $\mu$ ) of  $0.001\,\text{kg/m.s.}^{[3]}$  The governing equation, provided in equation 1, results from the Navier-Stokes equation for incompressible flow and the Boussinesq approximation to account changes in density due to the temperature within the system boundary.

$$\rho \nu \cdot \nabla \nu = -\nabla p + \mu \cdot \nabla^2 \nu + \rho_0 g \beta \left( T - T_{ref} \right) \tag{1}$$

In the above equation,  $\rho$  is the fluid density,  $\nu$  is the fluid velocity,  $\rho$  is the fluid pressure,  $\beta$  is the volume expansion coefficient, T is the fluid temperature, and  $T_{ref}$  is the reference temperature.

The full eye setup and verification thereof were conducted in a previous study.<sup>[25]</sup> The normal eye model was also compared with an experimental study using particle image velocimetry.<sup>[26]</sup> The comparison displayed similarities in the flow fields, providing confidence in the current model setup. This model will further be used to simulate 3 glaucoma filtration surgeries: trabeculectomy, NPDS, and mNPDS with a membrane peel. For all these cases, steady and laminar flow is assumed with rigid nonslip corneal walls.

### 2.2. Surgical simulation scenarios

The glaucomatous eye model was modified to include a Kelly punch incision (deep to approximately 50% thickness scleral flap) with a diameter of 0.8 mm to simulate a typical trabeculectomy procedure. Surgically, the Kelly punch is used to perform a sclerostomy, producing a clean cut through the TM to allow for adequate drainage of the aqueous humor.

As part of the trabeculectomy procedure, an iridectomy is commonly performed. This allows some of the aqueous humor to bypass the flow path around the iris and drain directly through the Kelly punch incision. The iridectomy is performed by cutting a section of the iris no smaller than 2 mm<sup>[27]</sup> (an approximate length of 2.2 mm was selected for this case), resulting in an inverse triangular incision. For ease

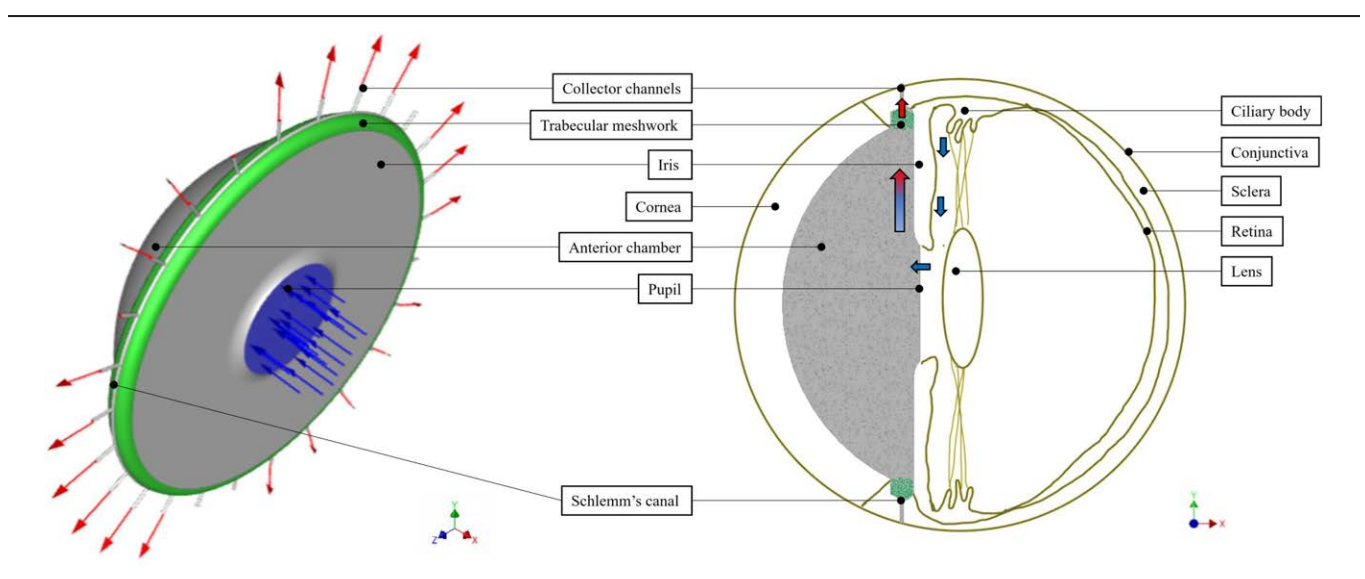


Figure 1. Anterior segment flow domain (gray) extracted from the idealized eye geometry including the pupil (aqueous humor inlet), anterior chamber, TM, SC, and collector channels (aqueous humor outlet). The aqueous humor inlet flow is indicated in blue and the outlet flow through the TM (green) is indicated in red. SC = Schlemm canal, TM = trabecular meshwork.

of simulation, the iridectomy was modeled as circular with a hydraulic diameter of 1.27 mm<sup>2</sup>, which was calculated using the equation

$$D_{ID} = \frac{a}{\sqrt{3}} \tag{2}$$

where *a* is the side length of an equilateral triangle. The geometry is illustrated in Figure 2, with the orange arrow indicating the flow through the sclerostomy.

The boundary conditions for the inlet mass flow rate (5E-08 kg/s), collector channel outlets (7 mm Hg), and TM permeability (4.34E-16 m²) are the same as for the glaucomatous model previously described. To simulate the immediate postoperative results, the Kelly punch is assumed to be open to the atmosphere. Thus, the boundary condition at the outlet of the Kelly punch is set to 0 mm Hg gauge pressure.

The NPDS procedural geometry includes the removal of the scleral flap (deep sclerectomy) as well as the deroofing of the SC. The deep sclerectomy is a  $4 \times 4$  mm excision of deep scleral tissue (deep to a 50% thickness superficial scleral flap) that is removed to access the canal of Schlemm and to allow for a "scleral lake" where aqueous humor may collect. At the anterior extent of the sclerectomy, the SC is deroofed to expose the JCT. The dissection may then be continued into the peripheral cornea. The superficial scleral flap is left in situ thus the aqueous humor is allowed to drain from the sides of the superficial flap. The flap is sutured; however, the purpose of the sutures is to keep the flap in situ rather than create tension as is the case with trabeculectomy. The conjunctiva is sealed over the scleral flap. As with the trabeculectomy procedure, the deep flap outlet area is exposed to atmospheric conditions before suturing occurs. The flow domain is illustrated in Figure 3, along with an XY-planar cross-sectional view of the eye. The SC deroofing section is illustrated in the enlarged view (red region) on the right of Figure 3.

The mNPDS procedure includes removing a small section of the JCT region of the TM. At the edges of where the SC was deroofed, an incision is made at a depth of 20 µm. [28] The membrane is then detached along the length of the SC deroofing area and extracted.

Once again, the superficial scleral flap is placed over the deep sclerectomy site before suturing takes place. The flow domain geometry is then similar to what is shown in Figure 3.

Additionally, suturing will be simulated by increasing the incision outlet pressure from 0 mm Hg to 7 mm Hg for each case, which will restore tension to the anterior chamber by creating resistance to flow. No clinical data were found that expressly indicate the pressure resistance of eye sutures. Since the exact outlet pressure resulting from sutures is not known, a value of 7 mm Hg was selected under the assumption that the suture pressure should be close to the original outlet pressure of the collector channels before the operation. However, this may vary depending on suture tightness and surgical technique. By simulating the sutures, it may be possible to indicate the post-operative IOP.

### 2.3. Mesh quality and convergence testing

No statistical analyses were conducted, as this was a deterministic simulation study. However, a mesh independence study was performed using IOP as the monitor variable, and a change of <1% was used as the convergence criterion. A sensitivity test was also conducted on the assumed suture pressure to assess the effect of varying suture outlet pressure from 0 to 10 mm Hg. Across all surgical types, IOP increased predictably with increasing suture tightness, confirming that suture pressure is a key modulator of postoperative outcomes.

A steady-state solver was employed using the SIMPLE algorithm for pressure-velocity coupling. Convergence was achieved when the residuals for all variables fell below  $1\times10^{-4}$ . For the CFD simulations, a tetrahedral mesh was selected to account for the complex geometry of the eye, illustrated on the left of Figure 4. This mesh would ensure the most accurate solution with the fewest elements. [29] Body sizing with a smooth transition inflation mesh was applied for all cases. To ensure that the CFD results were independent of the mesh, a mesh independence study was conducted with the IOP as the monitor value. The mesh was deemed acceptable when the error in the IOP value changed by <1%, as shown in Figure 4.

The mesh for the trabeculectomy case resulted in 4645,559 cells with an acceptable average mesh skewness and aspect ratio of 0.22 and 1.87, respectively.<sup>[30]</sup> The mesh for the NPDS cases resulted in 4956,830 cells with an acceptable average mesh skewness and aspect ratio of 0.21 and 2.11, respectively.

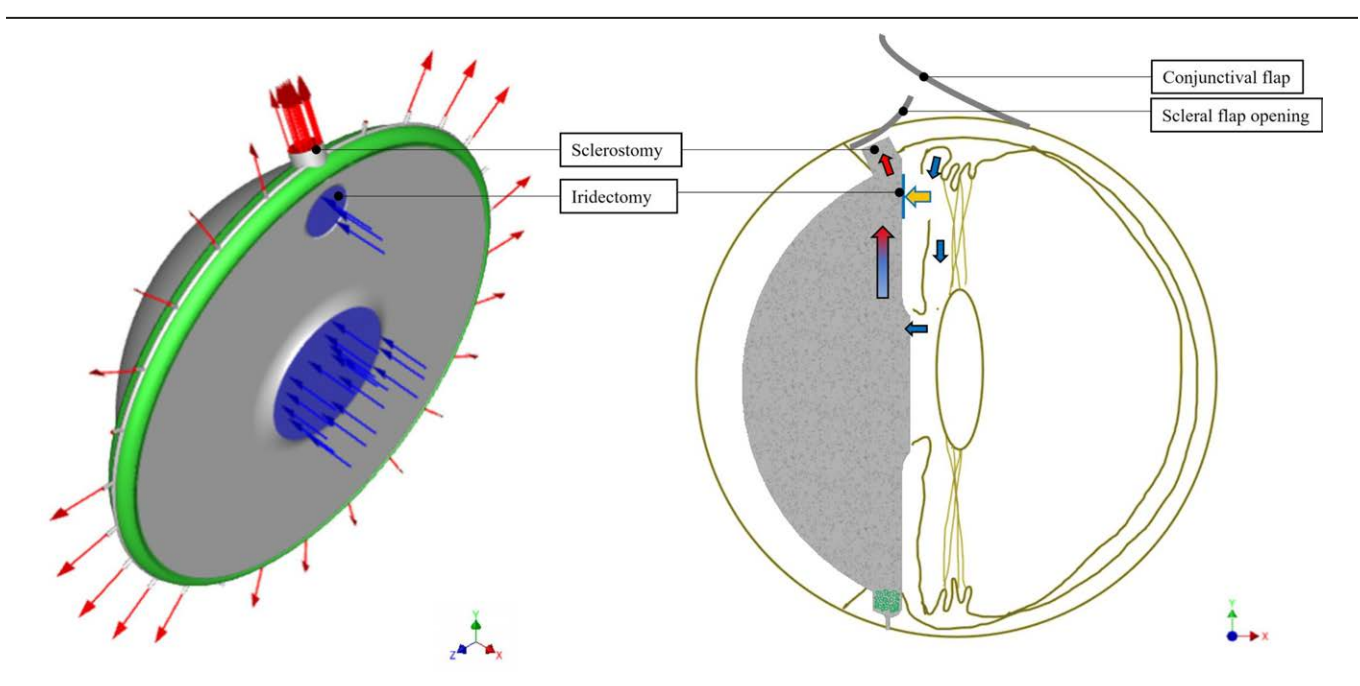


Figure 2. Anterior segment flow domain (gray) extracted to simulate trabeculectomy including the pupil and iridectomy (aqueous humor inlet), anterior chamber, TM, SC, and collector channels and sclerostomy (aqueous humor outlet). The aqueous humor inlet flow is indicated in blue and the outlet flow through the TM (green) is indicated in red. The orange arrow indicates the flow through the sclerostomy. SC = Schlemm canal, TM = trabecular meshwork.

A sensitivity analysis was conducted for suture pressure. While other parameters such as fluid viscosity and episcleral venous pressure were held constant based on literature values, future studies could investigate the impact of varying these parameters to further assess model robustness.

### 3. Results

For the CFD simulation of each surgical case, the postoperative IOP before and after suturing was examined. For each case, a preoperative glaucomatous IOP of 27 mm Hg was prescribed. [25] Table 1 describes the results. The postoperative IOP before suturing for trabeculectomy resulted in 0.007 mm Hg. This low value is expected, as the Kelly punch removes a section of the TM through its entire depth, drastically reducing the aqueous outflow resistance.

For the NPDS procedure, the IOP reduces to 20 mm Hg once the deep flap is generated, and the SC has been deroofed. In this case, the outlet area has been increased to allow for additional outflow, but no effort has been made to decrease the TM resistance. Thus, a reduction in IOP is experienced, though not as considerably as seen for trabeculectomy. Table 1 further depicts the resulting IOP for the mNPDS procedure, with the removal of the top layer of the TM. In this case, the IOP is reduced to 3.3 mm Hg before suturing. As with the NPDS procedure, the aqueous outflow area is increased with the additional step of reducing the TM resistance by incorporating the membrane peel.

A pressure value of 7 mm Hg was applied to the surgical area to ensure stable outflow, though it is possible to adjust the suture tension based on expert observations. Once this pressure is applied, the IOP will increase as the aqueous outflow area is restricted for each case. The resulting IOP following trabeculectomy is 7 mm Hg, which corresponds with another CFD model study for trabeculectomy (resulting IOP of 7.1 mm Hg).<sup>[3]</sup> Thus, the IOP has been reduced by 74.1%.

The postoperative IOP for NPDS is shown to be 23.4 mm Hg, signifying a decrease of 13.3%. As the steady-state IOP is above 21 mm Hg, the NPDS procedure would be deemed unsuccessful. Therefore, this case seems to support those studies claiming that

NPDS tends to be ineffective. However, if the membrane peel is performed during the procedure, the IOP would reduce to 6.98 mm Hg. These results indicate that mNPDS achieved an IOP outcome comparable to trabeculectomy, while NPDS without membrane peel was substantially less effective.

Immediate postoperative IOP reduction is only one factor in glaucoma surgical procedure success. [23,31] Since the present study does not take time into account (or consider conjunctival bleb formation and healing), only the steady-state results were evaluated to investigate the effectiveness of each surgical case.

Figure 5 further illustrates the velocity flow patterns of aqueous humor in sutured postoperative scenarios for each procedure, further providing insight into the aqueous humor flow dynamics and highlight the impact of surgical modifications on IOP reduction.

The trabeculectomy simulation reveals a velocity acceleration towards the surgical outlet. This is consistent with the removal of the TM and the direct pathway between the anterior chamber and the external drainage site. The high flow rates demonstrate the effectiveness of trabeculectomy in reducing outflow resistance and achieving significant IOP reduction.

The NPDS simulation demonstrates a more constrained flow pattern compared to trabeculectomy. Without the removal of the TM layer, resistance to outflow persists, resulting in slower velocity magnitudes and less effective drainage. This supports the study's findings that NPDS alone is less effective in lowering IOP, as the limited flow through the deroofed SC does not compensate for the resistance imposed by the TM.

The mNPDS simulation shows a marked improvement in flow dynamics compared to NPDS. The removal of the JCT layer significantly increases flow velocity near the surgical site, reducing overall resistance and achieving IOP outcomes comparable to trabeculectomy. This finding reinforces the study's conclusion that the membrane peel is a critical component of mNPDS success.

While a full analysis of streamline behavior and spatial variations is beyond the scope of this paper, these results highlight procedure-dependent differences in local flow dynamics.

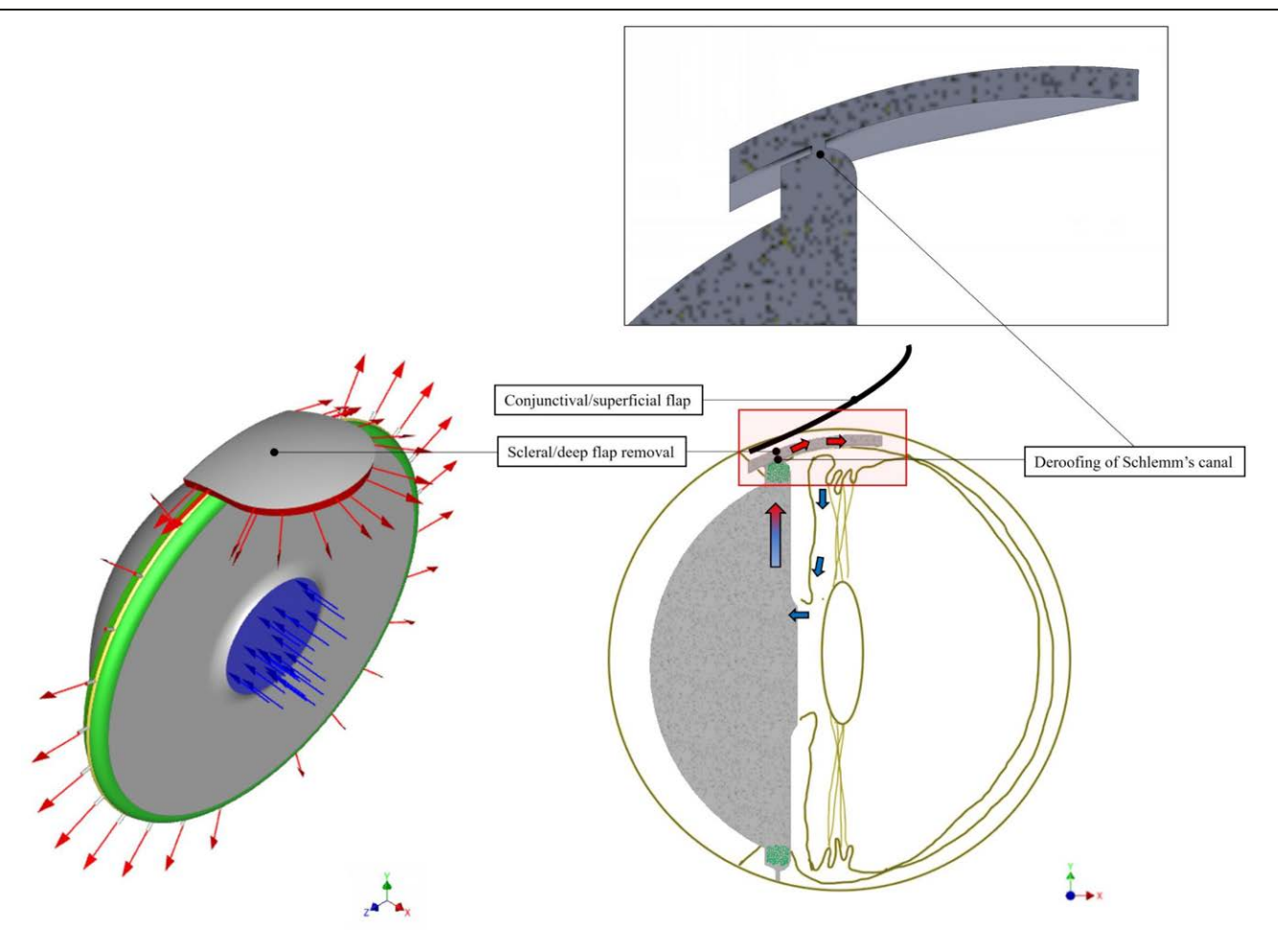


Figure 3. Anterior segment flow domain extracted to simulate NPDS including the pupil (aqueous humor inlet), anterior chamber, TM, SC, and collector channels and scleral flap removal (aqueous humor outlet). The aqueous humor inlet flow is indicated in blue and the outlet flow through the TM (green) is indicated in red. NPDS = nonpenetrating deep sclerectomy, SC = Schlemm canal, TM = trabecular meshwork.

# 4. Discussion

This study aimed to compare the immediate postoperative intraocular pressure outcomes of trabeculectomy, NPDS, and mNPDS using CFD simulations. The ongoing debate on the efficacy of NPDS may be attributed to the lack of specification in clinical studies regarding the membrane peel during the NPDS procedure.

Table 2 compares CFD-derived postoperative IOP values to those reported in clinical studies. In a clinical study comparing NPDS with mNPDS, it was noted that NPDS, with an average preoperative IOP of 24.22 mm Hg, resulted in a 1-day postoperative IOP of 19.0 mm Hg ± 6.7. [17] Applying this preoperative IOP to the CFD model yielded a postoperative IOP of 22.2 mm Hg, aligning closely with the clinical findings. This alignment enhances confidence in the validity of the surgical model and underscores the importance of clarifying the role of the membrane peel in NPDS procedures for accurate evaluation.

The same clinical study also reported that mNPDS, with an average preoperative IOP of 25.8 mm Hg, resulted in a 1-day postoperative IOP of 12.2 mm Hg ± 2.5.<sup>[17]</sup> In comparison, a trabeculectomy featuring an average preoperative IOP of 18.9 mm Hg showed an average 1-day postoperative IOP of 10.9 mm Hg. Simulating the preoperative IOP for these mNPDS and trabeculectomy scenarios, the CFD models produced postoperative IOP values of 6.98 mm Hg and 7 mm Hg, respectively. While the clinical and CFD studies present divergent numerical outcomes, both studies affirm that trabeculectomy and mNPDS

procedures are anticipated to result in a similar postoperative IOP. The velocity flow patterns observed in the simulations further confirm the critical role of the membrane peel in enhancing aqueous humor outflow and achieving effective IOP reduction, particularly in mNPDS. Since the JCT layer of the TM is known to be a major site of outflow resistance in the conventional aqueous pathway, the membrane peel supports the improved IOP-lowering effect seen in the mNPDS simulation. Eliminating this low-porosity layer facilitates a more direct and less resistive flow route into the subconjunctival space. Overall, the CFD model results suggest that modifications to the NPDS procedure can exert a considerable influence on the ultimate postoperative IOP.

Although the percentage reduction in IOP for NPDS is lower in the CFD model, the absolute postoperative value of 22.2 mm Hg falls within the reported clinical range of  $19.0 \pm 6.7$  mm Hg. This overlap supports the plausibility of the NPDS simulation. For mNPDS and trabeculectomy, the CFD results align with the clinical trend of greater IOP reduction, highlighting comparable effectiveness between the 2 procedures. While these CFD-derived postoperative IOP values differ numerically from clinical outcomes, partly due to uncertainty in modeling suture outlet pressure, the relative effectiveness of each surgical procedure is preserved. Both trabeculectomy and mNPDS result in substantially lower IOP compared to NPDS, consistent with the clinical trends observed in the referenced study.

The simulation results presented in this study exhibit a correlation with the findings from clinical studies, reinforcing the utility

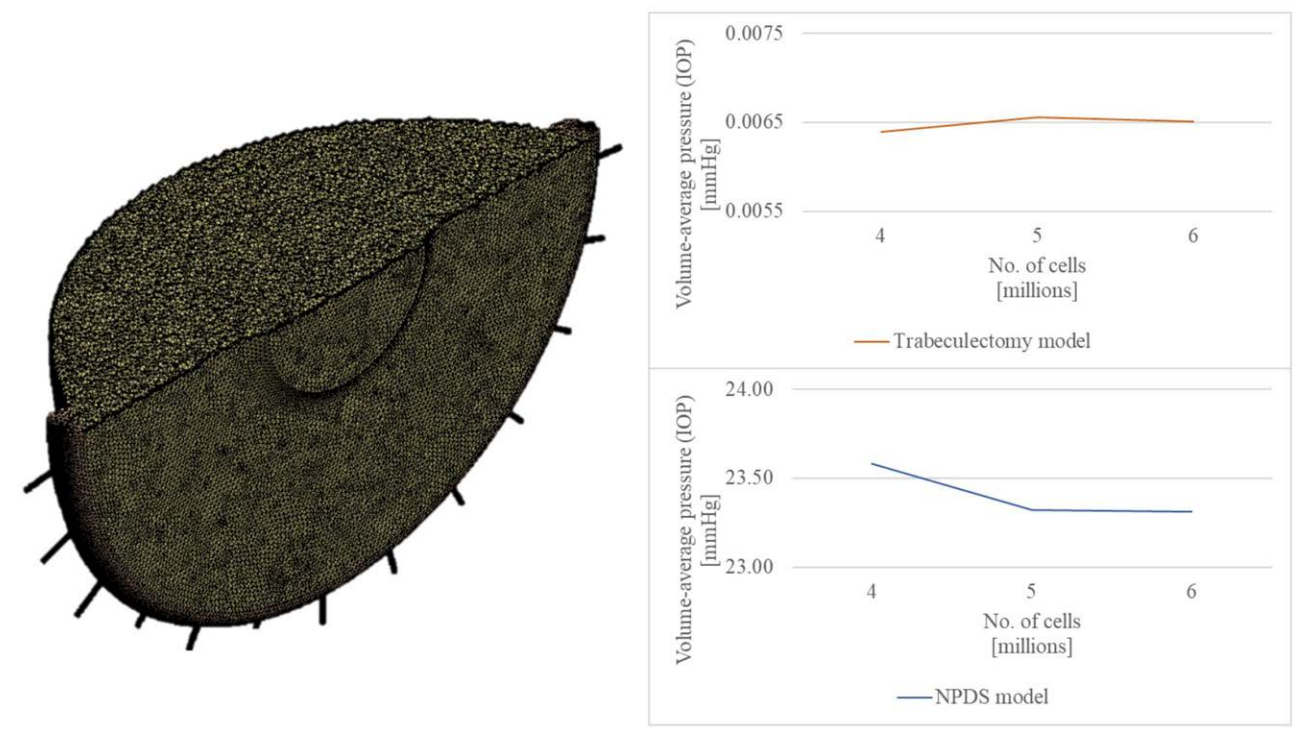


Figure 4. Trabeculectomy mesh display (left) and results of mesh independence study for trabeculectomy (top right) and NPDS (bottom right) model geometries. NPDS = nonpenetrating deep sclerectomy.

# Table 1

# IOP results before and after suturing for each filtration surgery (preoperative IOP = 27 mm Hg).

	IOP before suturing (mm Hg)	IOP after suturing (mm Hg)	
Trabeculectomy	0.007	7.00	
NPDS	20.43	23.40	
mNPDS	3.30	6.98	

IOP = intraocular pressure, mNPDS = modified nonpenetrating deep sclerectomy, NPDS = nonpenetrating deep sclerectomy.

of the computational model as a valuable tool for in-depth exploration of glaucoma procedures. While the simulated IOP values do not precisely match clinical measurements, the relative trends between procedures are consistent with clinical outcomes. These discrepancies are largely attributable to uncertainty in estimating suture outlet pressure, which is not directly measurable in vivo and varies substantially between surgeries. Notably, the simulated postoperative intraocular pressure IOP values for trabeculectomy and mNPDS align with the corresponding outcomes reported in clinical investigations. Despite numerical variations, both the clinical studies and the CFD model consistently project a comparable reduction in IOP for all 3 procedures. This congruence between simulated and clinically observed outcomes underscores the model's capacity to provide insights into the immediate postoperative efficacy of various glaucoma surgeries. The alignment between simulation and clinical results lends credence to the notion that CFD modeling can serve as a reliable preliminary tool for predicting surgical outcomes, offering a cost-effective and timeefficient means to assess the effectiveness of glaucoma procedures before embarking on extensive clinical trials. While simulation results align with clinical trends, these findings should be interpreted cautiously due to model assumptions and the lack of in vivo validation.

While CFD proves to be a valuable tool for informing surgical procedures, it is essential to acknowledge its inherent challenges and limitations in comparison to clinical studies. Specifically, the idealized model used in this study avoids the complexity of

patient-specific geometries, which are challenging to obtain and reproduce, and access to accurate data is also limited. Variations in trabecular height, corneal thickness, and eye diameter among individuals could introduce discrepancies between the simulated scenarios and real-world conditions. Additionally, the TM resistance parameters in the eye model may differ from those in clinical studies, affecting the accuracy of simulation outcomes. The surgical geometries were based on published anatomical data and surgical literature, but were not directly validated through imaging or measurement. However, the model's plausibility is supported by alignment between simulated IOP outcomes and those reported in clinical studies. Expert ophthalmologic input was consulted during the modeling process to guide the surgical modifications and ensure that they aligned with typical surgical practice.

Notably, suturing tightness represents a critical parameter prone to errors, given that suture pressure is not routinely measured during surgical procedures. In the absence of precise measurements, the estimated suture pressure in the models introduces a degree of uncertainty. Nevertheless, the flexibility to adjust suture pressure during simulations offers a degree of control over aqueous outflow, contributing to the adaptability and potential refinement of the CFD model. Additional limitations include the exclusion of inter-patient variability, as well as healing and long-term bleb modeling, which are factors that are currently beyond the scope of first-step CFD simulations. These limitations underscore the need for cautious interpretation of

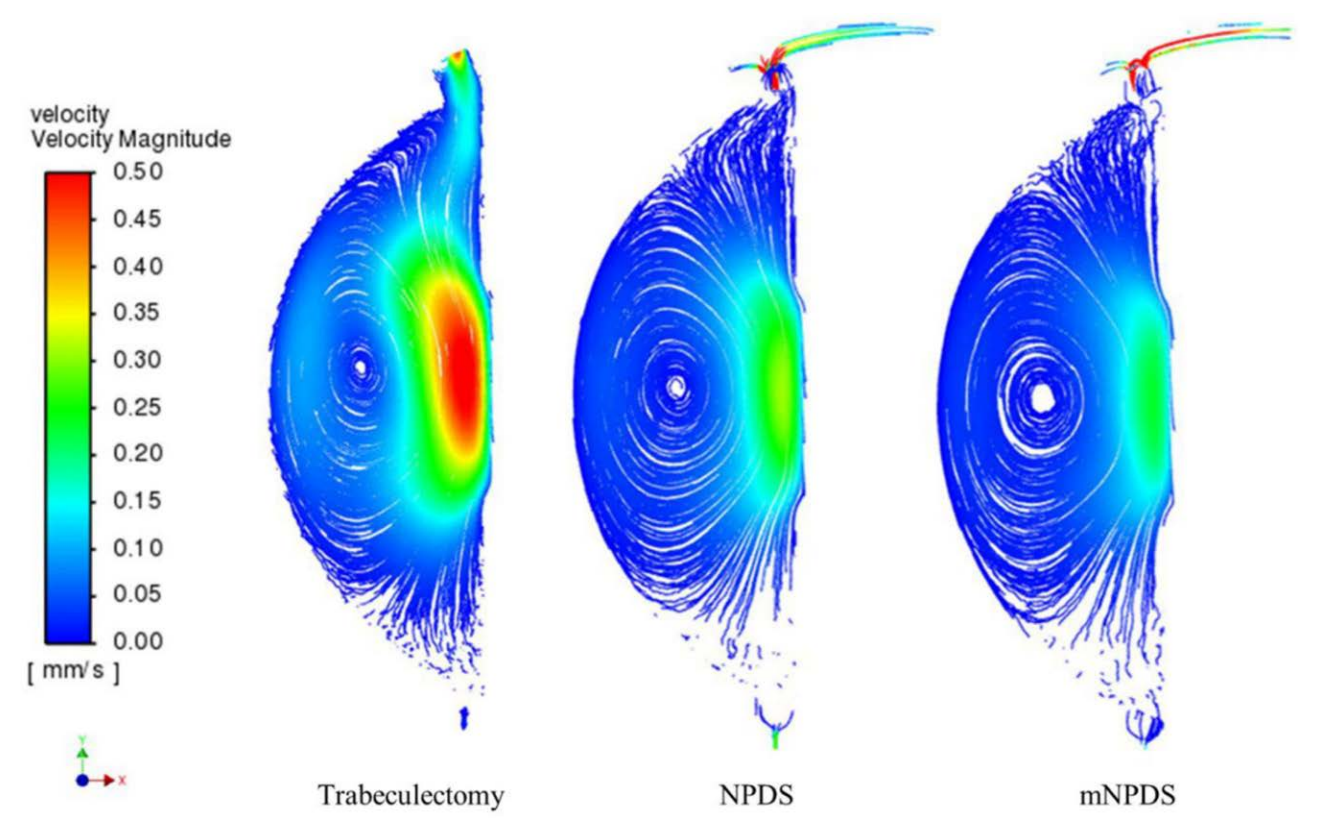


Figure 5. Velocity magnitude and flow patterns of aqueous humor for trabeculectomy (left), NPDS middle, and mNPDS (right). mNPDS = modified nonpenetrating deep sclerectomy, NPDS = nonpenetrating deep sclerectomy.

Table 2
Comparison of CFD-simulated postoperative IOP values with clinical data for trabeculectomy, NPDS, and mNPDS.

	Preoperative IOP [mm Hg]	CFD post-op IOP [mm Hg]	Clinical post-op IOP [mm Hg]	% IOP reduction (CFD)	Qualitative match
Trabeculectomy	18.9	7.0	10.9	63.0	Consistent trend
NPDS	24.22	22.22	$19.0 \pm 6.7$	8.3	Within clinical range
mNPDS	25.8	6.98	$12.2 \pm 2.5$	72.9	Consistent trend

CFD = computational fluid dynamics, IOP = intraocular pressure, mNPDS = modified nonpenetrating deep sclerectomy, NPDS = nonpenetrating deep sclerectomy.

CFD results and emphasize the complementary role of clinical studies in validating and refining modeling outcomes for a comprehensive understanding of glaucoma surgical procedures. Despite its limitations, the model highlights the potential for CFD to assist in presurgical decision-making once adapted for patient-specific anatomical inputs.

The main purpose of the study was to test the immediate postoperative efficacy of competing glaucoma filtration surgeries using CFD as the main tool of study. A 3D model of an eye with idealized geometry was presented and employed to simulate 3 different types of glaucoma surgeries namely trabeculectomy, NPDS and mNPDS. The resulting IOP values directly following the surgery (incisions open to atmosphere) and upon suturing were provided.

This comparative computational study employing CFD has provided valuable insights into the immediate postoperative efficacy of glaucoma filtration surgeries, specifically trabeculectomy, NPDS, and mNPDS. The CFD simulations demonstrated promising results in assessing IOP and immediate postoperative reduction rates for each surgical procedure. Notably, trabeculectomy and mNPDS displayed effectiveness in achieving an appropriate postoperative IOP, while NPDS showed limited efficacy. Although NPDS without the

membrane is no longer a standard that is used, the choice remains that of the surgeon.

The greatest advantage of this comparative CFD study is its ability to compare surgical outcomes without the interference of inter-individual variations. The CFD models were able to mimic results similar to those expected from clinical procedures, successfully showcasing the potential of CFD as a virtual tool for evaluating and comparing glaucoma surgical procedures.

CFD models possess the capability to function as digital twins with heightened clinical relevance through the incorporation of patient-specific or demographically representative geometric characteristics in a facile manner. Although this approach may differ from clinical outcomes, future studies will expand this CFD model to include diverse anatomical geometries, enhancing its clinical relevance. Additionally, a more comprehensive understanding of corneal biomechanics and postoperative scarring effects could be achieved by integrating CFD with finite-element analysis. This collaborative approach would contribute to a more accurate representation of real-world conditions and improve the predictive capabilities of the CFD model. Despite these challenges, the current study demonstrates the potential of CFD as a preliminary tool for evaluating

glaucoma surgical outcomes and warrants further exploration and validation through collaboration with clinical trials and additional refinement of the modeling approach.

# **Acknowledgments**

The authors gratefully acknowledge that the simulations presented in this paper were made possible using the Wits CFD cluster.

### **Author contributions**

Conceptualization: Nicol Basson, Susan Williams, Weihua Ho. Formal analysis: Nicol Basson.

Funding acquisition: Nicol Basson, Weihua Ho.

Investigation: Nicol Basson.

Methodology: Nicol Basson, Patrick Geoghegan, Susan Williams, Weihua Ho.

Supervision: Patrick Geoghegan, Susan Williams, Weihua Ho.

Validation: Nicol Basson. Visualization: Nicol Basson.

Writing - original draft: Nicol Basson.

Writing - review & editing: Nicol Basson, Patrick Geoghegan, Susan Williams, Weihua Ho.

### References

- [1] Lusthaus JA, Khatib TZ, Meyer PAR, McCluskey P, Martin KR. Aqueous outflow imaging techniques and what they tell us about intraocular pressure regulation. Eye. 2020;35:216–35.
- [2] Mauro A, Mohamed S. Three dimensional heat and mass transfer in human eye based on porous medium approach. Int J Heat Mass Transfer. 2020;158:119994.
- [3] Villamarin A, Roy S, Hasballa R, Vardoulis O, Reymond P, Stergiopulos N. 3D simulation of the aqueous flow in the human eye. Med Eng Phys. 2012;34:1462–70.
- [4] Gozawa M, Takamura Y, Aoki T, Iwasaki K, Inatani M. Computational fluid dynamics (CFD) simulation analysis on retinal gas cover rates using computational eye models. Sci Rep. 2021;11:1–8.
- [5] Coroneo MT, Graterol-Nisi G, Maver Ê, Gillies RM. Aqueous humor circulation in the era of minimally invasive surgery for glaucoma. Ann Biomed Eng. 2023;52:898–907.
- [6] Ou Y. Glaucoma surgery series: trabeculectomy. Brightfocus Foundation. 2021. https://www.brightfocus.org/glaucoma/article/glaucoma-surgery-series-trabeculectomy. Accessed July 18, 2022.
- [7] Pantalon A, Feraru C, Tarcoveanu F, Chiselita D. Success of primary trabeculectomy in advanced open angle glaucoma. Clin Ophthalmol. 2021;15:2219–29.
- [8] Sharifipour F, Yazdani S, Asadi M, Saki A, Nouri-Mahdavi K. Modified deep sclerectomy for the surgical treatment of glaucoma. J Ophthalmic Vis Res. 2019;14:144–50.
- [9] Cillino S, Di Pace F, Casuccio A, et al. Deep sclerectomy versus punch trabeculectomy with or without phacoemulsification: a randomized clinical trial. J Glaucoma. 2004;13:500–6.
- [10] Rulli E, Biagioli E, Riva I, et al. Efficacy and safety of trabeculectomy vs nonpenetrating surgical procedures: a systematic review and meta-analysis. JAMA Ophthalmol. 2013;131:1573–82.
- [11] Elewa L, Hamid M. Deep sclerectomy versus subscleral trabeculectomy in glaucomatous eyes with advanced visual field loss. J Egypt Ophthalmol Soc. 2014;107:277.

- [12] Sangtam T, Roy S, Mermoud A. Outcome and complications of combined modified deep sclerectomy and trabeculectomy for surgical management of glaucoma: a pilot study. Clin Ophthalmol. 2020;14:795–803.
- [13] Walkden A, Mercieca K, Perumal D, Anand N. Primary glaucoma surgery in Fuchs' heterochromic uveitis: a comparison of trabeculectomy versus deep sclerectomy. Ther Adv Ophthalmol. 2019;11:251584141986976.
- [14] Mokbel TH, Ghanem AA, Moawad AI, Nafie EM, Nematallah EH. Comparative study of phacoemulsification-subscleral trabeculectomy versus phacoemulsification-deep sclerectomy. Saudi J Ophthalmol. 2009;23:189–96.
- [15] Cheng JW, Cheng SW, Cai JP, Li Y, Wei RL. Systematic overview of the efficacy of non penetrating glaucoma surgery in the treatment of open angle glaucoma. Med Sci Monit. 2011;17:RA155–63.
- [16] Varga Z, Shaarawy T. Deep sclerectomy: safety and efficacy. Middle East Afr J Ophthalmol. 2009;16:123–6.
- [17] Kitsos G, Aspiotis M, Alamanos Y, Psilas K. A modified deep sclerectomy with or without external trabeculectomy: a comparative study. Clin Ophthalmol. 2010;4:557–64.
- [18] Bhartiya S, Ichhpujani P, Shaarawy T. Surgery on the trabecular meshwork: histopathological evidence. J Curr Glaucoma Pract. 2015;9:51–61.
- [19] Klemm M. Tiefe sklerektomie: eine alternative zur trabekulektomie. Ophthalmologe. 2015;112:313–8.
- [20] Kozobolis V, Panos GD, Konstantinidis A, Teus M, Labiris G. Modified deep sclerectomy combined with Ex-PRESS filtration device versus trabeculectomy for primary open angle glaucoma. Int J Ophthalmol. 2017;10:728–32.
- [21] Elhofi A, Helaly HA. Non-penetrating deep sclerectomy versus trabeculectomy in primary congenital glaucoma. Clin Ophthalmol. 2020;14:1277–85.
- [22] Heinz C, Koch JM, Heiligenhaus A. Trabeculectomy or modified deep sclerectomy in juvenile uveitic glaucoma. J Ophthalmic Inflamm Infect. 2011;1:165–70.
- [23] Eldaly MA, Bunce C, ElSheikha OZ, Wormald R. Comparison of two surgical techniques for the control of eye pressure in people with glaucoma. Cochrane. 2014. https://www.cochrane.org/CD007059/ EYES\_comparison-of-two-surgical-techniques-for-the-control-of-eyepressure-in-people-with-glaucoma. Accessed August 11, 2020.
- [24] Karimi A, Razaghi R, Stanik A, et al. High-resolution modeling of aqueous humor dynamics in the conventional outflow pathway of a normal human donor eye. Comput Methods Programs Biomed. 2025;260:108538.
- [25] Basson N, Alimahomed F, Geoghegan PH, Williams SE, Ho WH. An aqueous humour fluid dynamic study for normal and glaucomatous eye conditions. In: 2022 44th Annual International Conference of the IEEE Engineering in Medicine & Biology Society (EMBC). IEEE; 2022:3963–6.
- [26] Wang W, Qian X, Li Q, et al. Experimental study of aqueous humor flow in a transparent anterior segment phantom by using PIV technique. Mol Cell Biomech. 2019;16:59–74.
- [27] Spierer O, Cavuoto KM, Suwannaraj S, McKeown CA, Chang TC. Outcome of optical iridectomy in Peters anomaly. Graefes Arch Clin Exp Ophthalmol. 2018;256:1679–83.
- [28] Keller KE, Acott TS. The juxtacanalicular region of ocular trabecular meshwork: a tissue with a unique extracellular matrix and specialized function. J Ocul Biol. 2013;1:3.
- [29] ANSYS, Inc. ANSYS FLUENT 12.0 User's Guide 6.1.3 Choosing the Appropriate Mesh Type. https://www.afs.enea.it/project/neptunius/ docs/fluent/html/ug/node164.htm. Accessed January 22, 2022.
- [30] ANSYS, Inc. ANSYS FLUENT 12.0 User's Guide 6.2.2 Mesh Quality. https://www.afs.enea.it/project/neptunius/docs/fluent/html/ug/ node167.htm. Accessed January 22, 2022.
- [31] Bhartiya S, Dhingra D, Shaarawy T. Revisiting results of conventional surgery: trabeculectomy, glaucoma drainage devices, and deep sclerectomy in the era of MIGS. J Curr Glaucoma Pract. 2019;13:45–9.